INTERNATIONAL JOURNAL OF HYDROGEN ENERGY 50 (2024) 175–185

Available online at www.sciencedirect.com

ScienceDirect

journal homepage: www.elsevier.com/locate/he

Resilience-oriented placement of multi-carrier microgrids in power systems with switchable transmission lines

A. Rezaee Jordehi [a,*], *Seyed Amir Mansouri* [b], *Marcos Tostado-Véliz* [c], *Amir Ahmarinejad* [d], *Francisco Jurado* [c]

[a] Department of Electrical Engineering, Rasht Branch, Islamic Azad University, Rasht, Iran

[b] Institute for Research in Technology (IIT), ICAI School of Engineering, Comillas Pontifical University, 28015 Madrid, Spain

[c] Department of Electrical Engineering, University of Jaén, 23700 Linares, Spain

[d] Department of Electrical Engineering, Central Tehran Branch, Islamic Azad University, Tehran, Iran

HIGHLIGHTS

- Heat-power-hydrogen microgrids (MG's) are used to improve power system resilience.
- Resilience-oriented optimal placement of MGs has been done.
- Transmission line switching is used to improve the resilience of power systems.
- The effect of the number of MGs on power system resilience is assessed.
- Sensitivity of system resilience to MG-power system exchange limit is assessed.

ARTICLE INFO

Article history:
Received 1 April 2023
Received in revised form
2 July 2023
Accepted 24 July 2023
Available online 16 August 2023

Keywords:
Power system resilience
Microgrids
Transmission switching
Heat-power-hydrogen microgrids

ABSTRACT

Extreme events such as floods, hurricanes, earthquakes, and wildfires pose significant threats to the uninterrupted supply of electricity to consumers, as they can cause the failure of numerous power system components. The resilience of a power system is defined by its ability to withstand extreme events and continue meeting demand. While the placement of multi-carrier microgrids (MGs) in power systems can impact resilience, the literature lacks research on resilience-oriented placement. This paper aims to address this gap by proposing a resilience-oriented placement strategy for multi-carrier MGs, utilizing switchable transmission lines to enhance the resilience of power systems. The study focuses on a heat-power-hydrogen MG that obtains gas from a gas network, exchanges power with the main power system, and incorporates combined heat and power (CHP), electrolyzer, and thermal storage. The developed model employs a stochastic mixed-integer linear programming (MILP) approach, ensuring the attainment of the global optimum. Resilience is evaluated using the metric of expected load not supplied (ELNS). The results demonstrate that when the bus connected to the MG is isolated, the MG generates electricity through its CHP unit to meet local demand, reducing the total demand shed in the power system and improving system resilience. Specifically, the MG reduces ELNS from 4955.48 MWh to 2356.64 MWh, indicating a remarkable 52% improvement in ELNS.

* *Corresponding author*. Rasht Branch, Islamic Azad University, Rasht, Iran.
E-mail address: ahmadrezaeejordehi@gmail.com (A. Rezaee Jordehi).

https://doi.org/10.1016/j.ijhydene.2023.07.277

Furthermore, the study shows that transmission line switching further decreases ELNS from 2356.64 MWh to 848.68 MWh. Several experiments are conducted to analyze the sensitivity of power system resilience to the number of MGs, the MG-power system exchange limit, and the limit on gas import from the gas network.

Nomenclature

Sets

damaged	Set of damaged lines
$\Lambda_m^{connect}$	Set of buses connected to bus m
Λ_m^{g}	Set of generators at bus m

Bars

$\overline{*}$, $\underline{*}$	Upper and lower bounds

Indices

s	Scenario
t	Time
m, n	Bus
g	Generator
MG	MG
elec	Electric
ther	Thermal
hy	dr Hydrogen
CHP	CHP
TES	TES
charge/discharge	Charging/discharging mode of TES
electrolyzer	Electrolyzer
gas	Gas
MGimport	Power imported from power system to MG
OS	Open switches
shed	Shed

Parameters and variables

ρ	Auxiliary parameter for linearisation in line switching (a big positive number)
ν	Variable which is 1 for closed switches and zero for open switches
ω	Probability (of considered scenarios)
M	A big positive number (in CHP model)
N	Total number of MGs/open switches)
$\alpha, \beta, \gamma, \delta$	Vertices of feasible operating region of CHP
Rup	Ramp-up limit
Rdown	Ramp-down limit
η	Efficiency/coefficient of performance (for storage systems, CHP and electrolyzer)
conex	A parameter which is assigned 1 for connected buses
Demand	Demand
X	Reactance of transmission lines
ψ	Online/offline status
El	Energy level (of TES)
P	Electric power
TP	Thermal power
HP	Hydrogen power
PF	Flow (of lines)
θ	Phase angle of bus voltage
totalshed	Total load shed (for scenarios)
ELNS	Expected load not supplied
φ	A variable which is assigned 1 for buses connected to MG

1. Introduction

The uninterrupted supply of electricity as a critical service is of utmost importance for consumers. Extreme events such as flood, hurricane, windstorm, ice-storm, earthquake and wildfire are serious threats for uninterrupted supply of electricity consumers as they may result in severe failure of power system components. The increasing rate of the climate change is increasing the frequency and severity of extreme events [1]. In Nov. 8, 2022, in the northeast region of US, wildfire caused the failure of a hook carrying a conductor and resulted in $17 billion damage, including 85 death and 804 lost persons [2]. In 2017, power outages caused by hurricanes Harvey, Irma and Maria in US resulted in an economic loss of $22 billion [3]. In February 2021, the ice-storm in Texas, US caused 25 GW demand shed and left 405 million consumers unsupplied for two days [3].

Resilience may be defined as the ability of a power system to resist extreme events and continue supply of demands. Resilience of power systems is of high importance and must be considered in their operational planning and expansion planning [4,5]. There are diverse strategies for resilience enhancement of power systems; the first group of strategies includes hardening strategies which decrease the probability of damage of power system components during extreme events. The second group includes operational resilience enhancement strategies such as reconfiguration, repair crew scheduling and generation scheduling. Resilience enhancement strategies may be preventive or corrective.

In [6], a preventive methodology has been proposed for resilience enhancement against windstorms; the methodology considers tree-caused failures in distribution networks. The states of tees are categorised into healthy, uprooted, stem-breakage and branch-breakage states. In the proposed methodology, windstorm forecasts and data of trees and distribution branches are collected, the fragility curve of the overhead structures are constructed and in each time interval, a Markov model is developed for trees; finally, the vulnerable branches are identified and optimal islands are determined in a way to optimise the resilience of the distribution network. The uncertainties of demands have been considered in the proposed methodology.

In [7], optimal capacity of distributed generators and optimal location of microgrids (MGs) as well as reconfiguration have been used to enhance the resilience of distribution networks. The demands have been classified into high-priority, medium-priority and low-priority divisions. The studied MG includes both dispatchable and renewable energy resources. A robust method has been used for dealing with the uncertainties of renewable energy resources. To understand the basics and concepts of microgrid, the interested reader may refer to Refs. [8–12]. In Ref. [13], mobile generators, reconfiguration and scheduling of repair crew have been used for resilience improvement of distribution networks in a mixed-integer linear programming (MILP) framework. In Ref. [14], in a chance-constrained stochastic model, reconfiguration and MG formation have been used for resilience improvement of distribution networks. In Ref. [15], repair crew scheduling and reconfiguration have been used as corrective measures against hurricane to enhance distribution system resilience.

In [2], both hardening and operational strategies have been used for resilience enhancement of distribution networks against wildfires. The proposed strategy includes investment in distributed energy resources, storage systems as well as repair crew scheduling, generation scheduling, reconfiguration and mobile distributed energy resources. Prior to wildfire, camera networks with assistance of machine learning tools, detect wildfire and after wildfire detection, its propagation behavior is assessed. By geographic information system (GIS), the distance between wildfire and conductors or transformers is estimated and the impact of wildfire is assessed. If a portion of the system is expected to be islanded, the operator manages the system in a way that the islanded demands are fed by the formed microgrids.

In [16], the impact of electric vehicles (EVs) on resilience of electric distribution systems and transportation systems have been investigated; as per the achieved results, EVs improve the resilience of both electric and transportation systems. The barriers for using EVs in resilience enhancement have been identified. In Ref. [17], in a two-stage stochastic framework, the usage of EVs and scheduling of multi-MGs have been proposed for resilience enhancement of distribution networks, while different MGs are located in different regions with different climate. Ref [18] has conducted resilience-oriented planning of distribution systems by investment on distributed generators and hardening of lines. Authors in Ref. [19] have proposed a resilience enhancement strategy against wildfires; in the proposed strategy, the spatiotemporal characteristics of wildfires have been incorporated into generation scheduling model and a Markov decision process is used to find optimal generation dispatch at each time, as the wildfire propagates across the distribution system.

In [20], liquid natural gas (LNG) trailers and power system reconfiguration have been used to enhance the resilience of interconnected power-gas networks against windstorms. During windstorms, the gas hydrates, caused by low temperatures, may block gas sources and gas pipelines; this may interrupt the supply of gas demands in some gas nodes and may also shut-down gas-fired generators in power system and therefore impact both power and gas systems. In the proposed model, LNG trailers are optimally dispatched and LNG transported by trailers is delivered to LNG storage in gas distribution network for emergency gas supply. Online traffic information is used for optimal dispatch of trailers. The results show that LNG trailers restore more than 50% of electric demand and more than 60% of gas demand.

Considering the literature, to the best of the authors' knowledge, the resilience-oriented placement of multi-carrier MGs has not been done in the literature, while their location in power systems may affect the resilience of the system; therefore, in this paper, the main objective is to do resilience-oriented placement of multi-carrier MGs, moreover, transmission line switching is used as a measure to enhance the resilience of power systems. A modified IEEE 24-bus power system is used as case study; the studied MG includes combined heat and power (CHP), thermal energy storage (TES) and electrolyzer and supplies electric, thermal and hydrogen demands. The contributions of this paper are as follows.

- Multi-carrier MGs have been used to improve the resilience of power systems against hurricanes.
- Resilience-oriented optimal placement of MGs has been done.
- Transmission line switching has been used to improve the resilience of power systems.
- The effect of the number of MGs on power system resilience has been assessed.
- The sensitivity of power system resilience to the exchangeable power between power system and MG as well as importable gas from gas network has been assessed.

The paper is organised as below; the proposed model is introduced in the second section. The results and their analysis may be found in the third section and section 4 includes the conclusions of the paper.

2. Formulation of the model

As stated before, the case study is a modified IEEE 24-bus power system wherein the resilience-oriented placement of a heat-power-hydrogen MG is done. The developed stochastic MILP model is characterised by Constraints (1)–(8). See Fig. 1 which shows the studied MG-integrated IEEE 24-bus power system.

ELNS, which is the most common resilience metric, is used to quantify the resilience of the studied power system. It is defined by (1.a)-(1.b). According to (1.c), the demand shed at each bus, time and scenario is upper-bounded and may not exceed the demand in that bus, time and scenario.

$$ELNS = \sum_{s} \omega_s.totalshed_s \tag{1.a}$$

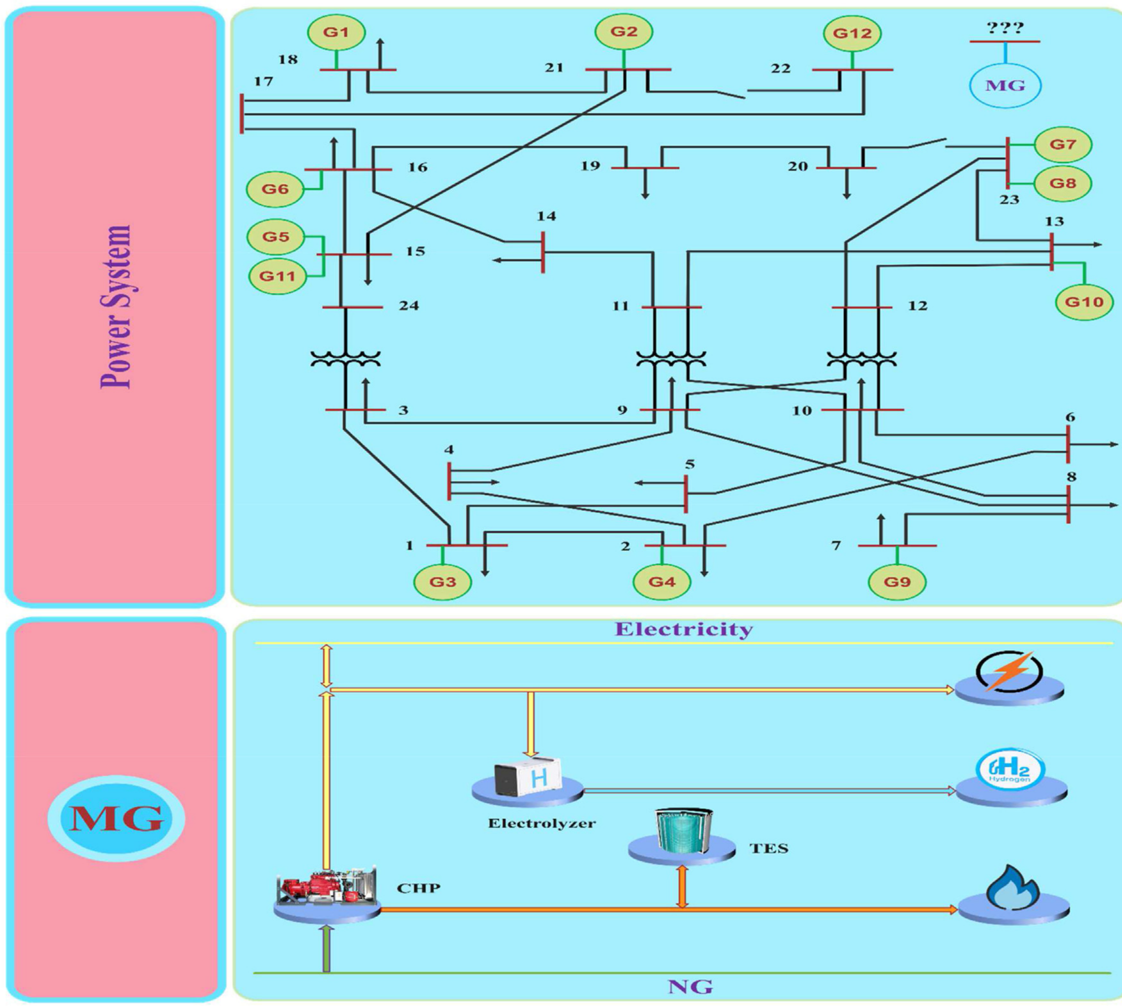

Fig. 1 – MG-integrated IEEE 24-bus power system.

$$totalshed_s = \sum_t \sum_m P_{shed,m,t,s} \, \forall s \tag{1.b}$$

$$0 \le P_{shed,m,t,s} \le \mathrm{Demand}_{m,t} \, \forall m, \, \forall t, \, \forall s \tag{1.c}$$

Power flow constraints, considering transmission line switching and MG placement, are as (2.a) to (2.j) [21]. Variable $\upsilon_{m,n,t,s}$ is 0 for open-switched transmission lines and 1 for close-switched transmission lines. According to (2.c), total number of open switches in power system must be equal to a prespecified value N_{OS}. As per (2.d), variables $\upsilon_{m,n,t,s}$ and $\upsilon_{n,n,t,s}$ are equal as they refer to the same transmission line. Constraints (2.e) indicate that the power flow of damaged lines is equal to zero. Constraints (2.f) impose upper bounds on power flow of transmission lines. Constraints (2.g) ensure power balance in system buses; according to (2.g), at each bus, time and scenario, sum of power of connected generators and demand shed should be equal to sum of demand, power export to MG and power outflows to the connected buses. Constraints (2.i) fix the phase angle of the reference bus at zero and constraint (2.j) ensures that the number of MGs placed in the power system is equal to the number of available MGs. For bus m, variable φ_m is 1 if and only if MG is placed in bus m.

$$PF_{m,n,t,s} - \left(\frac{\theta_{bus,t,s} - \theta_{node,t,s}}{X_{bus,node}}\right) \le \rho(1 - \upsilon_{m,n,t,s}) \, \forall (m,n) \in conex(m,n) \\ and \notin damaged(m,n,t,s), \, \forall t, \, \forall s \tag{2.a}$$

$$PF_{m,n,t,s} - \left(\frac{\theta_{bus,t,s} - \theta_{node,t,s}}{X_{bus,node}}\right) \ge -\rho(1 - \upsilon_{m,n,t,s}) \, \forall (m,n) \in conex(m,n) \\ and \notin damaged(m,n,t,s), \, \forall t, \, \forall s \tag{2.b}$$

$$\sum_n \sum_m (1 - \upsilon_{m,n,t,s}) = 2N_{OS} \tag{2.c}$$

$$\upsilon_{m,n,t,s} = \upsilon_{n,m,t,s} \, \forall (m,n) \in conex(m,n) \\ and \notin damaged(m,n,t,s), \, \forall t, \, \forall s \tag{2.d}$$

$$PF_{mn,t,s} = 0 \, \forall (m,n) \in damaged(m,n,t,s), \, \forall t, \, \forall s \tag{2.e}$$

$$\underline{PF_{m,n}} \le PF_{m,n,t,s} \le \overline{PF_{m,n}} \forall (m,n) \in conex(m,n) \\ and \notin damaged(m,n,t,s), \forall t, \forall s \tag{2.f}$$

$$\sum_{g \in \Lambda_m^g} P_{g,t,s} + P_{shed,m,t,s} = Demand_{m,t} + P_{MGimport,m,t,s} + \sum_{n \in \Lambda_m^{connect}} P_{m,n,t,s} \forall m, \forall t, \forall s \tag{2.g}$$

$$-\frac{\pi}{2} \le \theta_{m,t,s} \le \frac{\pi}{2} \forall m, \forall t, \forall s \tag{2.h}$$

$$\theta_{ref,t,s} = 0 \forall t, \forall s \tag{2.i}$$

$$\sum_m \varphi_m = N_{MG} \tag{2.j}$$

The operation of generators in power system must meet constraints (3.a) to (3.c) which include ramp-up/down limits as well as upper and lower limits on the generated power [22]. Ramp limits prevent sudden changes in power generation and avoid the mechanical stress on generators.

$$P_{g,t+1,s} - P_{g,t,s} \le Rup_g \forall g, t, s \tag{3.a}$$

$$P_{g,t-1,s} - P_{g,t,s} \le Rdown_g \forall g, t, s \tag{3.b}$$

$$\underline{P_g} \psi_{g,t,s} \le P_{g,t,s} \le \overline{P_g} \psi_{g,t,s} \forall g, \forall t, \forall s \tag{3.c}$$

Due to the capacity limit of the transformer connecting MG and power system, the electric power exchange between MG and power system is bounded as (4.a). Constraints (4.b) make sure that the gas import of MG from gas network does not exceed its limit.

$$-\overline{P_{MGimport}} \varphi_m \le P_{MGimport,m,t,s} \le \overline{P_{MGimport}} \varphi_m \forall m, \forall t, \forall s \tag{4.a}$$

$$P_{gas,t,s} \le \overline{P_{gas}} \forall t, \forall s \tag{4.b}$$

The balance of electricity, heat, hydrogen and gas in MG are respectively ensured through constraints (5.a) to (5.d). As per MGs electricity balance in (5.a), sum of electric power imported from power system and power produced by CHP must be equal to sum of MGs' electric demand and electric power fed into electrolyzer. As per MGs' heat balance in (5.b), sum of thermal power produced by CHP and releasing thermal power of TES should not be less than sum of MGs' thermal demand and charging thermal power of TES. As per MGs' hydrogen balance in (5.c), the hydrogen produced by electrolyzer should not be less than MGs' hydrogen demand. Finally, as per MGs' gas balance in (5.d), all imported gas is fed into CHP unit.

$$\sum_m P_{MGimport,m,t,s} + P_{CHP,t,s} = \left(\frac{HP_{electrolyzer,t,s}}{\eta_{electrolyzer}}\right) + Demand_{MG,elec,t,s} \forall t, \forall s \tag{5.a}$$

$$TP_{CHP,t,s} + TP_{TES,dch,t,s} \ge Demand_{MG,ther,t,s} + TP_{TES,charge,t,s} \forall t, \forall s \tag{5.b}$$

$$HP_{electrolyzer,t,s} \ge Demand_{MG,hydr,t,s} \forall t, \forall s \tag{5.c}$$

$$P_{gas,t,s} = \left(\frac{P_{CHP,t,s}}{\eta_{P,CHP}}\right) \forall t, \forall s \tag{5.d}$$

The studied MGs include CHP, electrolyzer and TES. Stochastic model of CHP may be found in (6.a) to (6.i). Constraints (6.a) to (6.d) ensure that the changes in heat and power of CHP does not exceed is ramp limits and constraints (6.e) to (6.i) make sure that the operating point of CHP is within its feasible operating region, specified by vertices $\alpha, \beta, \gamma, \delta$ [23].

$$P_{CHP,t+1,s} - P_{CHP,t,s} \le Rup_{CHP,P} \forall t, \forall s \tag{6.a}$$

$$P_{CHP,t-1,s} - P_{CHP,t,s} \le Rdown_{CHP,P} \forall t, \forall s \tag{6.b}$$

$$TP_{CHP,t+1,s} - TP_{CHP,t,s} \le Rup_{CHP,TP} \forall t, \forall s \tag{6.c}$$

$$TP_{CHP,t-1,s} - TP_{CHP,t,s} \le Rdown_{CHP,TP} \forall t, \forall s \tag{6.d}$$

$$0 \le P_{CHP,t,s} \le P_{CHP,\alpha} \cdot \psi_{CHP,t,s} \forall t, \forall s \tag{6.e}$$

$$0 \le TP_{CHP,t,s} \le TP_{CHP,\beta}\ \psi_{CHP,t,s} \forall t, \forall s \tag{6.f}$$

$$P_{CHP,t,s} - P_{CHP,\alpha} - \frac{(P_{CHP,\alpha} - P_{CHP,\beta})(TP_{CHP,t,s} - TP_{CHP,\alpha})}{TP_{CHP,\alpha} - TP_{CHP,\beta}} \le 0 \forall t, \forall s \tag{6.g}$$

$$P_{CHP,t} - P_{CHP,\beta} - \frac{(P_{CHP,\beta} - P_{CHP,\gamma})(TP_{CHP,t,s} - TP_{CHP,\beta})}{TP_{CHP,\beta} - TP_{CHP,\gamma}} \ge - M(1 - \psi_{CHP,t,s}) \forall t, \forall s \tag{6.h}$$

$$P_{CHP,t,s} - P_{CHP,\gamma} - \frac{(P_{CHP,\gamma} - P_{CHP,\delta})(TP_{CHP,t,s} - TP_{CHP,\gamma})}{TP_{CHP,\gamma} - TP_{CHP,\delta}} \ge - M(1 - \psi_{CHP,t,s}) \forall t, \forall s \tag{6.i}$$

Electrolyzer is an important MG component, which produces hydrogen to supply hydrogen demands. Similar to generators and CHP, according to (7.a) and (7.b), the increase in hydrogen production of the electrolyzer should not exceed its ramp-up limit and the decrease in its hydrogen production should not exceed its ramp-down limit. Moreover, as per (7.c), the hydrogen production of the electrolyzer must be within a pre-specified range.

$$HP_{electrolyzer,t+1,s} - HP_{electrolyzer,t,s} \le Rup_{electrolyzer} \forall t, \forall s \tag{7.a}$$

$$HP_{electrolyzer,t-1,s} - HP_{electrolyzer,t,s} \le Rdown_{electrolyzer} \forall t, \forall s \tag{7.b}$$

$$\underline{HP_{electrolyzer}} \psi_{electrolyzer,t,s} \le HP_{electrolyzer,t,s} \le \overline{HP_{electrolyzer}} \psi_{electrolyzer,t,s} \forall t, \forall s \tag{7.c}$$

Finally, the charge and discharge of TES as thermal storage component of MG must satisfy constraints (8.a) to (8.f) [22]. Constraints (8.a), (8.b) and (8.c) respectively confine the charging heat, discharging heat and energy level of TES within their corresponding pre-specified ranges. Constraints (8.d) ensure that the charge and discharge of TES does not happen simultaneously. Constraints (8.e) make sure that the initial and final energy level of TES are the same and (8.f) indicates how heat level of TES changes during charging and discharging times.

$$\underline{TP}_{TES,discharge}\psi_{TES,discharge,t,s} \leq TP_{TES,discharge,t,s} \leq \overline{TP}_{TES,discharge}\psi_{TES,discharge,t,s} \forall t, \forall s \tag{8.a}$$

$$\underline{TP}_{TES,charge}\psi_{TES,charge,t,s} \leq TP_{TES,charge,t,s} \leq \overline{TP}_{TES,charge}\psi_{TES,charge,t,s} \forall t, \forall s \tag{8.b}$$

$$\underline{El}_{TES} \leq El_{TES,t,s} \leq \overline{El}_{TES} \forall t, \forall s \tag{8.c}$$

$$\psi_{TES,charge,t,s} + \psi_{TES,discharge,t,s} \leq 1 \forall t, \forall s \tag{8.d}$$

$$El_{TES,end,s} = El_{TES,begining} \forall s \tag{8.e}$$

$$El_{TES,t,s} = El_{TES,t-1,s} + \eta_{TES,charge}TP_{TES,charge,t,s} - \frac{TP_{TES,discharge,t,s}}{\eta_{TES,discharge}} \forall t, \forall s \tag{8.f}$$

3. Results and analysis

In this section, the results of the introduced model on IEEE 24-bus power system are presented and analysed. Data of IEEE 24-bus power system can be found in Ref. [21]. In transmission line switching, it is assumed that at each time, two and only two switches are open. Resilience-oriented placement of a heat-power-hydrogen MG is conducted through a stochastic model. The studied multi-carrier MG gets gas from a gas network, exchanges power with power system and includes CHP, electrolyzer and TES. The maximum production of the electrolyzer is 30 MW, its efficiency is 80% and its ramp-up and ramp-down limits are both 10 MW/h. The maximum possible power exchange between power system and MG is 200 MW and the maximum importable gas from gas network is 500 MW. The peak of electricity, heat and hydrogen demands are 150 MW, 40 MW and 25 MW, respectively. Data of TES and CHP have been included in Tables 1 and 2, respectively. Throughout the paper, the default units for time, power and energy are hour (h), MW and MWh, respectively.

In the developed stochastic model for resilience enhancement against hurricanes, the uncertainties of the failed lines, hurricane starting time and the time taken to repair the failed lines are taken into account and the model is solved based on 10 reduced scenarios of Table 3. As the developed model is a MILP model, the achievement of the global optimum is guaranteed. The model is solved with CPLEX solver in general algebraic modeling system (GAMS) which is a commercial tool for optimisation models. Ten, as the number of scenarios has been chosen as a trade-off between accuracy and computational burden. Higher number of scenarios increases the accuracy of the model at the expense of higher computational burden.

The results of the developed model for resilience-oriented placement of MG in IEEE 24-bus power system shows that bus 19 is the optimal location for MG and ELNS is 2356.64 MWh. Looking at the scenarios in Table 3, we found that in scenario #1, due to the failure of lines 16–19, 19–20 and 20–23, buses 19 and 20 are islanded and in scenarios 2, 4, 5 and 8, due to the failure of lines 16–19 and 19–20, bus 19 is isolated; therefore, bus 19 seems to be a critical bus in this power system as it is in islanded mode in scenarios 1, 2, 4, 5 and 8. Conclusively, placing MG in bus 19 helps power system to supply the demand in this bus by local generation in scenarios 1, 2, 4, 5 and 8. Besides islanding of buses, transmission congestion is another potential reason for demand shed in power systems. The results show that demand shed exists only at buses 1, 5, 19 and 20. Demand shed at bus 19, in different scenarios have been shown in Fig. 2. It must be highlighted here that with probability 0.84, this bus goes into islanded mode and it is the most critical bus of the studied power system. Total demand shed of the system in different scenarios have been illustrated in Fig. 3 which shows that the studied power system experiences the highest demand shed in scenarios 1, 2, 5 and 8.

Fig. 4 illustrates the power exchange between power system and MG in different scenarios. According to this figure, in scenario 1 in which no failure occurs in transmission lines, MG imports electricity from power system, however in scenarios such as 1, 2, 5 and 8 in which bus 19 is islanded, the direction of power transfer is reversed; MG produces electricity with its CHP unit and supplies the local demand in bus 19, thereby total demand shed in power system decreases. The electric power which CHP produces in different scenarios, may be seen in Fig. 5. According to Fig. 5, in scenario 1 in which MG behaves as an electricity consumer, CHP is offline in most time periods and produces its minimum power in other times, however in scenarios such as 1, 2, 5 and 8 in which MG must feed the local demand, CHP increases its power production level to enable MG to feed local demand. Thermal power of CHP in different times and scenarios may be seen in Fig. 6. The thermal power production of CHP is affected not only by MGs heat demand, but also by its electric power production, as its operating point must be confined within a pre-specified feasible operating region.

A set of experiments has been conducted to find the sensitivity of ELNS with respect to the number of MGs, MG-power system exchange limit and the limit on gas import from gas network. Regarding the experiment to find the sensitivity of ELNS to the number of MGs, the results show that optimal placement of a single MG decreases ELNS from 4955.48 MWh to 2356.64 MWh, which indicates a 52% improvement in ELNS. Resilience-oriented placement of 2

Table 1 – Data of TES.

Initial energy	Minimum energy	Maximum energy	Minimum charging power	Maximum charging power	Minimum discharging power	Maximum discharging power	Charging efficiency	dis charging efficiency
15	5	30	0	3	0	3	0.95	0.95

Table 2 – CHP data.

Power ramp-up limit	Power ramp-down limit	Heat ramp-up limit	Heat ramp- down limit	α_p	α_h	β_p	β_h	γ_p	γ_h	δ_p	δ_h
100	100	100	100	290.4	0	243.2	196	54	138	64	150

Table 3 – Reduced scenarios.

Scenario	failed lines and their failure period	Weight
1	3-9, 18–21, 20–23 at times [5,20], 19–20, 11–14, 16–19 at times [1,24]	0.4
2	3-9, 18–21 at times [5,20], 19–20, 11–14, 16–19 at times [1,24]	0.2
3	1-2, 1–3, 5–10, 8–9 at times [5,20]	0.01
4	3-9, 16–19, 19–20 at times [5,20]	0.1
5	1-2, 1–3, 5–10 at times [5,20], 19–20, 16–19 at times [1,24]	0.03
6	3-9, 14–16 at times [5,20],	0.02
7	1-2, 1–3 at times [5,20], 14–16, 16–19 at times [1,24]	0.02
8	8-9, 15–16 at times [1,23], 19–20, 16–19 at times [1,24]	0.11
9	3-9, 19–20 at times [2,22]	0.1
10	No failure	0.01

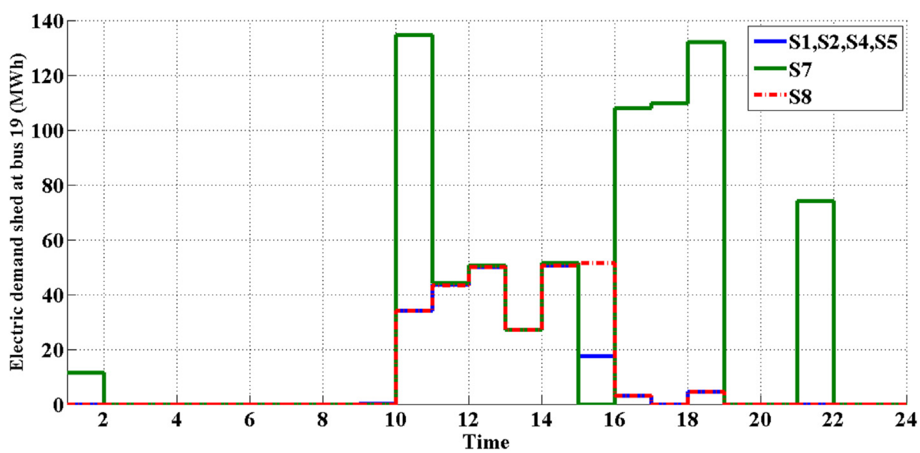

Fig. 2 – Electricity demand shed at bus 19.

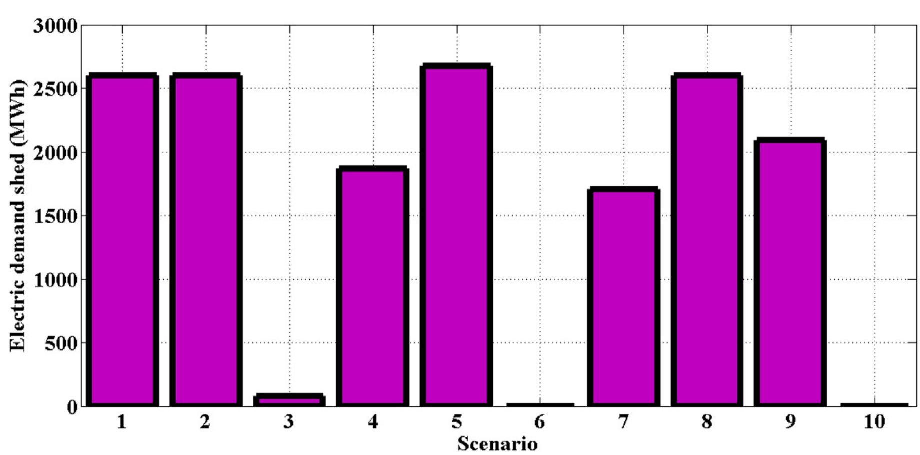

Fig. 3 – Total electricity demand shed at different scenarios.

identical MGs improve power system resilience by 72%, while buses 19 and 20 are found as optimal locations. Resilience-oriented placement of 3 identical MGs makes ELNS as low as 3.04 MWh, while buses 11, 19 and 20 are their optimal locations. With placement of 4 MGs in buses 1, 11, 19 and 20, the studied power system experiences no demand shed and its ELNS is equal to zero. See Fig. 7 which shows the relationship between ELNS and the number of MGs.

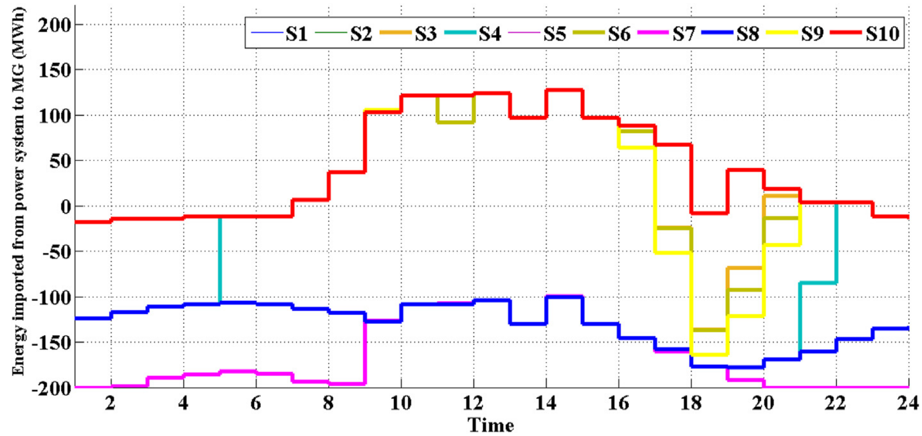

Fig. 4 — Electric power exchange between power system and MG.

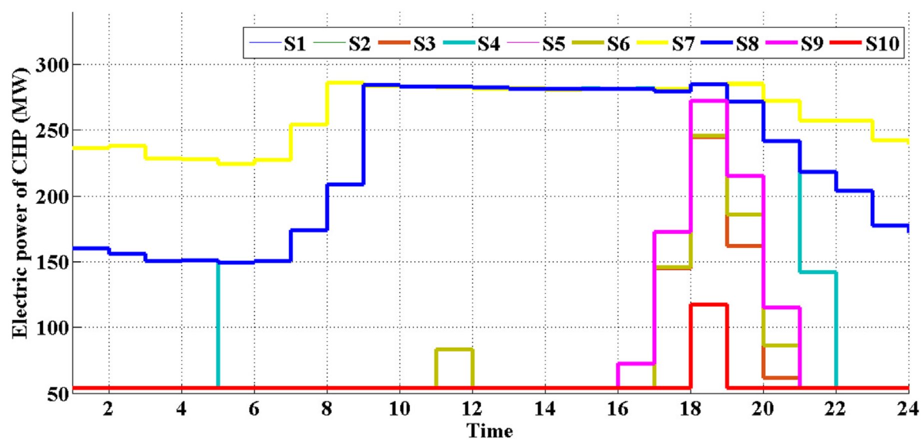

Fig. 5 — Electric power of CHP unit.

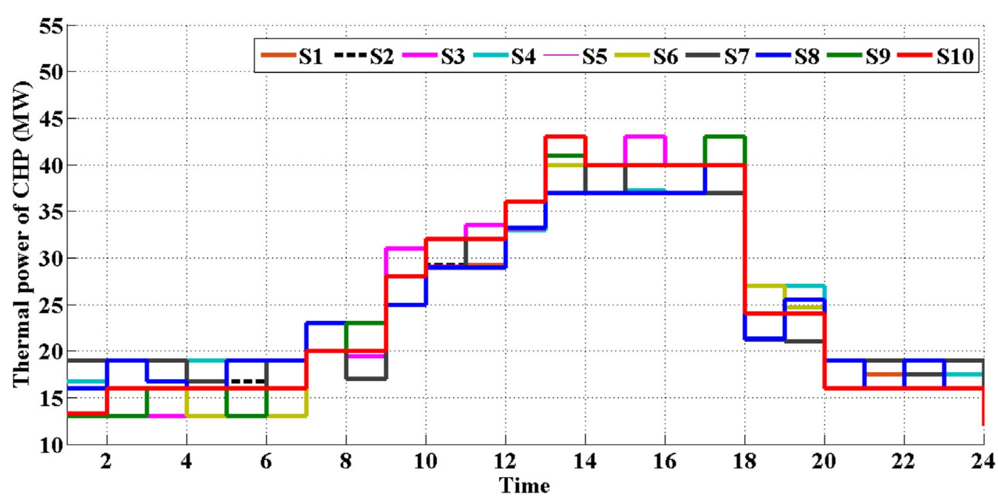

Fig. 6 — Thermal power of CHP unit.

Regarding the experiment to discover the sensitivity of ELNS to MG-power system exchange limit, the results show that ELNS is to some extent sensitive to this limit. When MG-power system exchange limit is as low as 50 MW, MG is only able to supply a small portion of local demand during bus islanding and ELNS is as high as 3857.21 MWh; doubling this limit and having 100 MW as MG-power system exchange limit, improves power system resilience by 24.3%.; doubling this limit again and having 200 MW as MG-power system exchange limit, improves power system resilience by 39%. The results

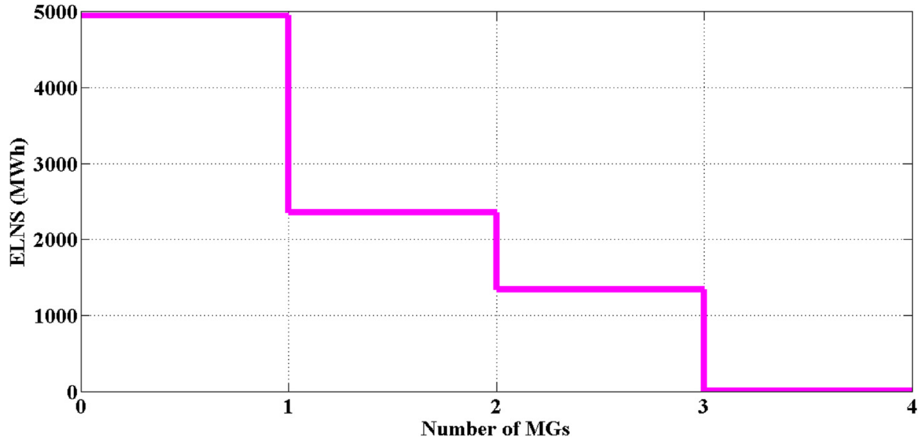

Fig. 7 – The relationship between ELNS and the number of MGs.

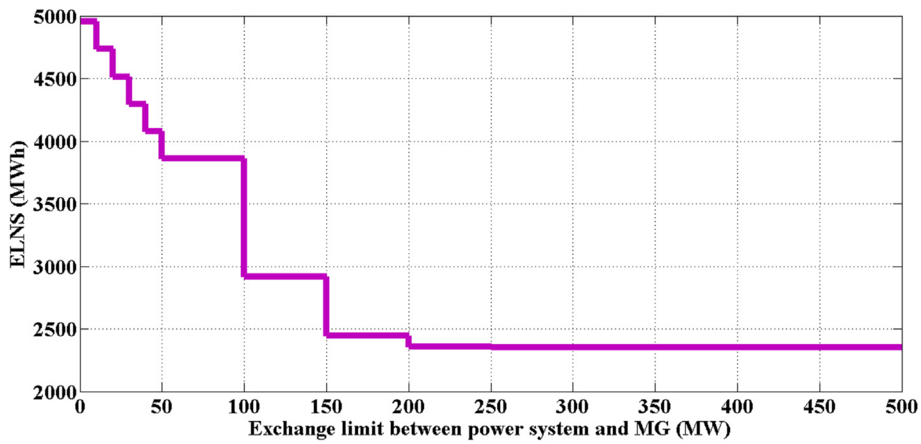

Fig. 8 – The relationship between ELNS and exchange limit of power system and MG.

imply that increasing MG-power system exchange limit beyond 250 MW does not lead to any change in power system resilience. Refer to Fig. 8 to see how ELNS changes with respect to MG power system exchange limit.

Regarding the experiments to find the impact of the gas import limit on ELNS, the results show that it significantly impacts ELNS and power system resilience. For low values of gas import limit, CHP unit as the sole electricity producer of MG has not enough gas input to fully supply the demand of power system at bus 19 in islanding scenarios, so a high ELNS value is resulted; for instance, if the gas import limit is 100 MW, ELNS is as high as 4952.96 MWh. For higher gas import limits, CHP is able to supply a higher portion of power system demand at bus 19 in islanding scenarios, so lower

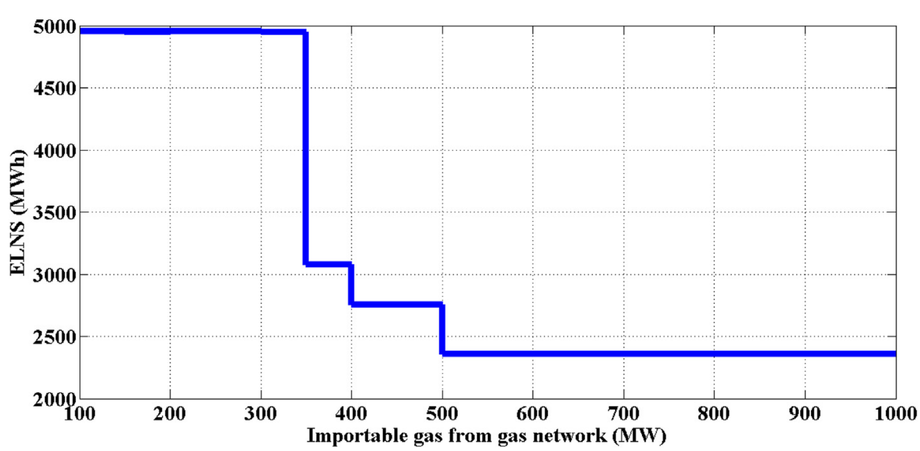

Fig. 9 – The relationship between ELNS and importable gas from gas network.

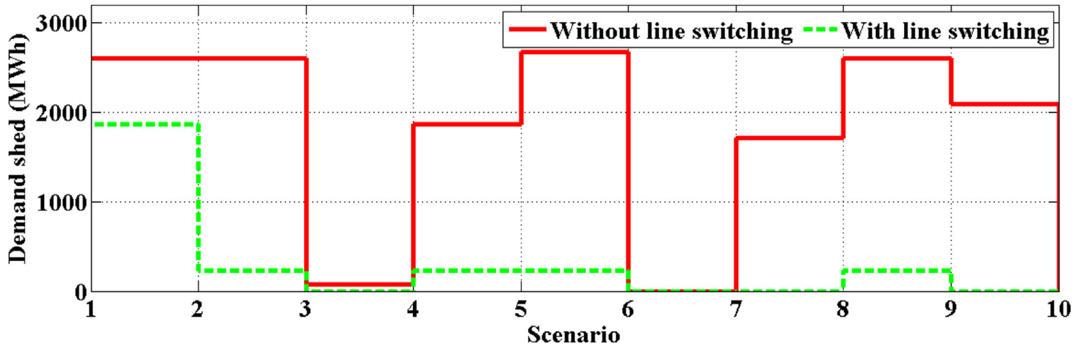

Fig. 10 – The effect of transmission line switching on demand shed at different scenarios.

ELNS is resulted; for instance, if gas import limit increases from 100 MW to 400 MW, ELNS decreases from 4952.96 MWh to 2753.40 MWh, which indicates 44% improvement in ELNS. For gas import limits of 500 MW and above, CHP is able to fully supply power system demand at bus 19 in islanding scenarios, so further increase of this limit does not lead to any improvement in ELNS and power system resilience. See Fig. 9 in which the relationship between ELNS and importable gas limit has been illustrated.

Here, the impact of transmission line switching on power system resilience is investigated. The number of open switches in the system is assumed 2. At each time and scenario, 2 and only 2 switches in the system should be open. The results show that transmission line switching decreases ELNS to 848.68 MWh. Using transmission line switching, demand shed at scenarios 1, 2, 4, 5 and 8 are respectively 1867.54 MWh, 231.05 MWh, 231.05 MWh, 231.05 MWh and 231.05 MWh and in other scenarios, no demand shed is required. See Fig. 10 which shows the effect of transmission line switching on demand shed. The figure clearly indicates positive impact of transmission line switching on ELNS and power system resilience. As an example, in scenario 1, demand shed has decreased from 2599.4 MWh to 1867.54 MWh.

4. Conclusions

In this paper, multi-carrier MGs and transmission line switching have been used to enhance the resilience of power systems against hurricanes. In the developed stochastic MILP model, the uncertainties of the failed lines, hurricane starting time and repair time have been considered. The model has been solved with CPLEX solver in general algebraic modeling system (GAMS) which is a commercial tool for solving optimisation models.

As per the achieved results, in scenarios in which no failure happens for transmission lines, MG imports electricity from power system, however in scenarios in which the bus connected to MG is islanded, the direction of power transfer is reversed; MG produces electricity with CHP unit and supplies the local power system demand, thereby decreases total demand shed and improves power system resilience. As per results, transmission line switching significantly improves power system resilience. A set of experiments have been conducted to find the sensitivity of power system resilience metric with respect to the number of MGs, MG-power system exchange limit and the limit on gas import from gas network.

The results show that optimal placement of a single MG reduces ELNS from 4955.48 MWh to 2356.64 MWh, which indicates a 52% improvement. Resilience-oriented placement of 2 identical MGs improve power system resilience by 72%. Resilience-oriented placement of 3 and 4 identical MGs make ELNS respectively 3.04 MWh and 0 MWh. The results show that MG-power system exchange limit significantly affects ELNS. When it is as low as 50 MW, MG may only supply a small portion of local demand during bus islanding and ELNS is as high as 3857.21 MWh; doubling this limit improves power system resilience by 24.3%., however, increasing MG-power system exchange limit beyond 250 MW does not lead to any improvement in power system resilience.

The results show that gas import limit significantly impacts power system resilience. For low values of gas import limit, CHP has not sufficient gas input to supply the whole power system demand at local bus in islanding scenarios, so relatively high ELNS values are resulted. For higher gas import limits, CHP is able to supply a higher portion of power system demand at local bus in islanding scenarios, so lower ELNS values are resulted. For gas import limits of 500 MW and above, CHP is able to supply the whole power system demand at local bus in islanding scenarios, so further increase of this limit does not lead to any improvement in ELNS and power system resilience.

Declaration of competing interest

The authors declare that they have no known competing financial interests or personal relationships that could have appeared to influence the work reported in this paper.

REFERENCES

[1] Bhusal N, Abdelmalak M, Kamruzzaman M, Benidris M. Power system resilience: current practices, challenges, and future directions. IEEE Access 2020;8:18064–86.

[2] Moreno R, Trakas DN, Jamieson M, Panteli M, Mancarella P, Strbac G, Marnay C, Hatziargyriou N. Microgrids against wildfires: distributed energy resources enhance system resilience. IEEE Power Energy Mag 2022;20:78–89.
[3] Shi Q, Liu W, Zeng B, Hui H, Li F. Enhancing distribution system resilience against extreme weather events: concept review, algorithm summary, and future vision. Int J Electr Power Energy Syst 2022;138:107860.
[4] Mansouri SA, Nematbakhsh E, Javadi MS, Jordehi AR, Shafie-khah M, Catalão JP. Resilience enhancement via automatic switching considering direct load control program and energy storage systems. In: 2021 IEEE international conference on environment and electrical engineering and 2021 IEEE industrial and commercial power systems europe. IEEE: EEEIC/I&CPS Europe); 2021. p. 1–6.
[5] Mansouri SA, Nematbakhsh E, Ahmarinejad A, Jordehi AR, Javadi MS, Marzband M. A hierarchical scheduling framework for resilience enhancement of decentralized renewable-based microgrids considering proactive actions and mobile units. Renew Sustain Energy Rev 2022;168:112854.
[6] Bahrami M, Vakilian M, Farzin H, Lehtonen M. A novel pre-storm island formation framework to improve distribution system resilience considering tree-caused failures. IEEE Access 2022;10:60707–24.
[7] Borghei M, Ghassemi M. Optimal planning of microgrids for resilient distribution networks. Int J Electr Power Energy Syst 2021;128:106682.
[8] Liu J, Cao X, Xu Z, Guan X, Dong X, Wang C. Resilient operation of multi-energy industrial park based on integrated hydrogen-electricity-heat microgrids. Int J Hydrogen Energy 2021;46:28855–69.
[9] Van LP, Do Chi K, Duc TN. Review of hydrogen technologies based microgrid: energy management systems, challenges and future recommendations. Int J Hydrogen Energy 2023;48(38):14127–48.
[10] Bovo A, Poli N, Trovò A, Marini G, Guarnieri M. Hydrogen energy storage system in a Multi–Technology Microgrid: technical features and performance. Int J Hydrogen Energy 2023;48(32):12072–88.
[11] Bayrak G, Küçüker A, Yılmaz A. Deep learning-based multi-model ensemble method for classification of PQDs in a hydrogen energy-based microgrid using modified weighted majority algorithm. Int J Hydrogen Energy 2023;48:6824–36.
[12] Nasir M, Jordehi AR, Tostado-Véliz M, Mansouri SA, Sanseverino ER, Marzband M. Two-stage stochastic-based scheduling of multi-energy microgrids with electric and hydrogen vehicles charging stations, considering transactions through pool market and bilateral contracts. Int J Hydrogen Energy 2023;48(61).
[13] Zeng Y, Qin C, Liu J, Xu X. Coordinating multiple resources for enhancing distribution system resilience against extreme weather events considering multi-stage coupling. Int J Electr Power Energy Syst 2022;138:107901.
[14] Biswas S, Singh MK, Centeno VA. Chance-constrained optimal distribution network partitioning to enhance power grid resilience. IEEE Access 2021;9:42169–81.
[15] Shi Q, Li F, Dong J, Olama M, Wang X, Winstead C, Kuruganti T. Co-optimization of repairs and dynamic network reconfiguration for improved distribution system resilience. Appl Energy 2022;318:119245.
[16] Hussain A, Musilek P. Resilience enhancement strategies for and through electric vehicles. Sustainable Cities and Society; 2022. p. 103788.
[17] Ebadat-Parast M, Nazari MH, Hosseinian SH. Distribution system resilience enhancement through resilience-oriented optimal scheduling of multi-microgrids considering normal and emergency conditions interlink utilizing multi-objective programming. Sustain Cities Soc 2022;76:103467.
[18] Shahbazi A, Aghaei J, Pirouzi S, Niknam T, Shafie-khah M, Catalão JP. Effects of resilience-oriented design on distribution networks operation planning. Elec Power Syst Res 2021;191:106902.
[19] Abdelmalak M, Benidris M. Enhancing power system operational resilience against wildfires. IEEE Trans Ind Appl 2022;58:1611–21.
[20] Li B, Chen Y, Wei W, Wang Z, Mei S. Online coordination of LNG tube trailer dispatch and resilience restoration of integrated power-gas distribution systems. IEEE Trans Smart Grid 2022;13:1938–51.
[21] Jordehi AR, Tabar VS, Jirdehi MA. A two-stage stochastic model for security-constrained market clearing with wind power plants, storage systems and elastic demands. J Energy Storage 2022;51:104550.
[22] Jordehi AR, Javadi MS, Catalão JP. Day-ahead scheduling of energy hubs with parking lots for electric vehicles considering uncertainties. Energy 2021;229:120709.
[23] Jordehi AR. Two-stage stochastic programming for risk-aware scheduling of energy hubs participating in day-ahead and real-time electricity markets. Sustainable Cities and Society; 2022. p. 103823.